Differential Thermal Inertia of Geological Surfaces

Don Sabol[a], Alan Gillespie[a], Eric McDonald[b], Iryna Danilina[a]

[a]Department of Earth & Space Sciences, Box 351310, University of Washington, Seattle, WA 98195
[b]Earth & Ecosystems Science, Desert Research Institute, 2215 Raggio Parkway, Reno, Nevada 89512

Introduction

In terrestrial remote sensing, thermal inertia has been little used because its calculation involves registered albedo, day-night TIR, and DEM images, and its value is sensitive to vegetation, transient cloudiness and wind. We explore a technique in which $\Delta T/\Delta t \approx dT/dt$ (the rate of temperature change) is measured and used to estimate thermal inertia. dT/dt is proportional to the day/night temperature difference, and hence *P*. It can be measured for short time intervals, reducing the opportunity for cloudiness, wind or rainfall to disrupt the experiment. It has its maximum/minimum values in the morning or afternoon, instead of noon/midnight for the conventional approach. These characteristics make for a better experimental design.

In the differential approach, however, ΔT is much smaller than in the day/night approach (~20ºK), and therefore $\Delta T/\Delta t$ is more sensitive to measurement precision (NEΔT). NEΔT is a more important limit to the ability to recover *P*, therefore. Essentially, Δt must be large enough that ΔT » NEΔT. For sensors such as MASTER, NEΔT ≈ 0.3 K, and common surfaces Δt > 60 minutes for a signal/noise ratio of 10 or more. Although such a low SNR may be acceptable in photointerpretation, it reduces the reliability of quantitative analysis of *P*; yet, increasing Δt further both reduces the pragmatic advantages of the differential approach and the ability to estimate dT/dt.

In this study, we use a FLIR Systems ThermaCAM S45 TIR camera to evaluate differential thermal inertia relative to day/night algorithms for a playa (Soda Lake) and environs in the Mojave Desert of California.

Background

Thermal Inertia

- Thermal inertia (*P*) is defined as:

  $$P = (kpC)^{1/2}$$

  where *k* = bulk thermal conductivity [cal s^{-1} cm^{-1} K^{-1}]; *p* = bulk density [g cm^{-3}]; *C* = specific heat capacity [cal g^{-1} K^{-1}]. It is generally estimated by comparing temperature differences at different times of day to values predicted by temperature diffusion models (Kahle, 1977). Typically, measurements are made near noon and midnight to maximize the contrast.

- A simpler approach yields an approximation of *P*, the apparent thermal inertia (*ATI*), which is determined using two temperature images, one made during the day (T_{day}) and one at night (T_{night}), and the surface albedo (Price, 1977):

  $$ATI = (1 - A)/(T_{day} - T_{night}) \qquad \text{where } A = \text{albedo}$$

- Thermal-inertia mapping (e.g., Gillespie and Kahle, 1977) is sensitive to differences in near-surface density, composition, and porosity.

Material	Typical Thermal Inertia
desert soils	~0.024 cal cm^{-2} K^{-1} s$^{-1/2}$
basalt	~0.053 cal cm-2 K-1 s$^{-1/2}$
water	~0.038 cal cm^{-2} K^{-1} s$^{-1/2}$

(Kahle, 1980)

An increase in soil moisture increases the thermal inertia of that soil as air in the pore spaces of the soil are (in part) replaced by water (Fig. 1).

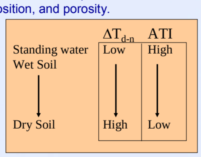

Figure 1. The effect of soil moisture on thermal inertia.

- Direct measurement of *P* is difficult because the values of *k*, *p*, and *C* for scene components are usually unknown and cannot be measured remotely. Remote determination of even relative thermal inertia is complicated by: 1) heterogeneity of materials in the instantaneous field of view; 2) topographic roughness; 3) moisture content; 4) vegetation; and 5) variable local weather conditions (temperature, cloud cover, rainfall, wind). *(Van Dam et al. 2005)*

Differential Thermal Inertia

- Materials with different thermal inertias have different diurnal temperature fluctuations, requiring that d*T*/*dt* also is different, at least at some times of day (Fig. 2). Therefore, *P* can be inferred from the rate of temperature change as well as from the daily min/max temperatures, with the notable difference that the optimum times of measurement are out of phase.

- Thermal radiance images can now be measured with precisions better than when the classic terrestrial thermal-inertia studies were made in the 1970s, and this improvement can be used to shorten Δt used while maintaining the same number of meaningful gray levels in the output *ATI* image. We call the *ATI* calculated with short Δt values "differential *ATI*," or *DATI*.

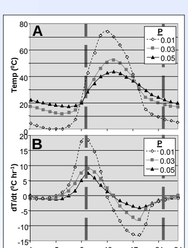

Figure 2. Changes in temperature (A) and the rate of temperature change over time (B) for different thermal inertia values (P).

Study Site

Soda Playa is at the terminus of the Mojave River and is seasonally wet during the year. The river itself is dry at the surface and provides subsurface moisture to parts of the western side of the playa. The surface of the playa is dominated by wind-blown silt that forms a surface crust. Evaporates form in these crusts (primarily sodium carbonate and sodium bicarbonate) and can locally dominate surface composition. In July, the crust of the playa surface is primarily dry, while the subsurface typically has moisture content up to 22% by weight.

Figure 3. Location of the study area.

Methods

- Thermal images were taken every 5 minutes in 10 second time bursts with an FSI FLIR camera from the Zzyzx Research Station located on the western edge of the playa over a diurnal period.

- Images were made of an area along the western edge of the playa (viewing toward the center of the playa) that included wet and dry patches. Four of these patches were instrumented with data loggers that recorded the subsurface temperature via thermocouples imbedded at depths of 2cm, 5cm, 10cm, and 40cm (Fig. 4).

- Moisture content of the subsurface at these depths was determined by weighing and drying samples collected at the same depths as the imbedded thermocouples at each "patch."

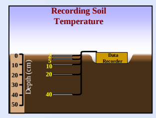

Figure 4: Diagram of thermocouple placement at sample sites.

- These 10 second time bursts were averaged to reduce the effective NEΔT of the FSI FLIR (0.2 K) from 0.2 K to ~0.06 K. By averaging these time bursts, we were able to calculate values of dT/dt that were relatively insensitive to fluctuating sensible-heat loss due to wind.

- The moisture content and subsurface temperatures were used to compare to the FLIR data as well as from theoretical results calculated from heat-diffusion equations.

Results

Subsurface Soil Moisture and Temperature

- The skin surface (down to at least 0.5 cm) of the playa in the analysis is dry (< 4% moisture by weight).

- Soil moisture under this "dry skin" can be as high as 18%, depending on the site and depth (Fig. 5).

- For the purposes of this study, "wet" and "dry" refer to the moisture content immediately under the surface (1 to 5 cm). Therefore, C and D are "wet" while A is "dry." Radiant, air, and subsurface soil temperatures at theses sites varied during the heating cycle with depth and composition (primarily moisture content). This can be seen in Figure 6, which contrasts the effect of wet and dry sub-surface soils on the morning heating.

- The intensity of the heat wave diminished with depth, such that the effect is only a few degrees at (40 cm) that occurs hours after initial heating.

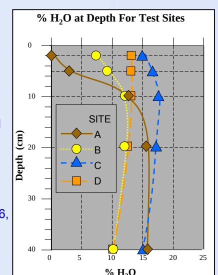

Figure 5. Sub-surface moisture content for four sites at Soda Playa.

- At the surface, the heating response is more immediate and intense. The increased moisture in the near-subsurface diminishes the rate and intensity of heating. It is the rate of heating at the surface/near-surface that is useful for short-term differential thermal inertia.

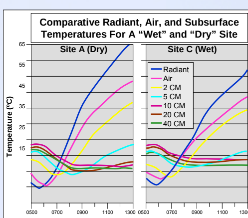

Figure 6. The effect of morning heating of soil at depth for Sites A and C. The radiant temperatures were extracted form a series of FLIR images while sub-surface temperatures were measured with thermocouples.

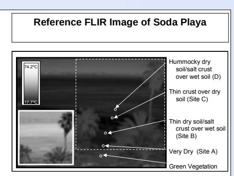

Figure 7. FLIR image of the view towards the east from Zzyzx Desert Studies Center overlooking Soda Lake Playa taken at 0540, 14 July, 2006. A photo of the area is inset and depicts the area shown by the dashed box in the FLIR image. This figure is presented as a reference for the time series of FLIR images shown in Figure 8.

Surface Radiant Temperature

- The short-term change in surface temperatures of dry and moist subsurface playa soils can be seen in thermal images. Figure 7 is a reference image for the time series shown in Figure 8.

- The left column of Figure 8 is a time series of FLIR images taken between 0600 and 0820 during morning sunrise taken every 20 minutes (the same day as Fig. 7). The difference between the FLIR image in Figure 7 (taken a 0540) and each subsequent time step is shown in the center column of Figure 8.

- The band of cooler soil in the lower center of the image (marked by an X) is relatively dry, powdery, and hummocky (relative to the surrounding playa surfaces). With its pore spaces filled with more air (as opposed to water), its thermal inertia is lower and, therefore, gets cooler at night..

- Progressive 20-minute temperature differences are shown in the right column of Figure 8. The top image is the difference between the 0540 and 0800 FLIR images and shows little change as the sun has not yet risen over the mountains to the east. A rapid rate of surface heating occurred between 0640 and 0700 (when the full sun has finally reached the whole scene).

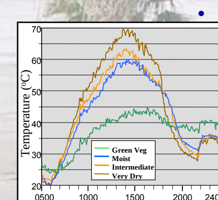

Figure 9: Non-smoothed temperature changes for different units form 0500 to midnight (every 5 minutes), 14 July 2006. The rate of temperature change is maximum (and less noisy) in the morning and late afternoon.

- Note that the cooler, hummocky area (X) is still warming at a slower rate (darker in Figure 8) than the surrounding wetter soil up until ~0740. This is counter to what might be expected. This dryer zone should be warming faster than the wetter playa as it has a lower *P* and, therefore, should respond faster to heating/cooling cycles. This apparent cooling is due to the fact that the image is taken looking east, towards the rising sun. The low sun angle in early morning causes shadows on the rough surface of this zone and the image is looking into those shadows. Hence, all the surfaces of this dry zone are not yet exposed to full sunlight / heating. As the sun continues to rise, this changes; and by 0820, the differential heating shows a relatively rapid temperature rise in this zone.

Figure 8: A Series of FLIR images taken from east to west across Soda Lake Playa, California, USA.

Conclusions

- Near-surface composition affects the response of surface to diurnal heating and cooling.

- Ideal measurement times - morning (from sunrise until ~ 0900) or in the evening (from just before subset until (~2100). It appears that a minimum of 20 minutes in desert environments is necessary, although closer to 2 hours would be ideal.

- Other factors: Surface roughness, wind, & clouds. can cause fluctuations in the surface temperature. Use multiple images (5 – 20) averaged over a 1-2 minute period to minimize these fluctuations.

- DATI has the potential to be used to map, and ultimately estimate thermal inertia. This approach shows promise in that it allows for relatively quick assessment of apparent thermal inertia and reduces affects of changes in climate, clouds, winds, etc. over traditional day/night methods. This makes it more adaptable for field analysis as well as use with unmanned airborne vehicles.

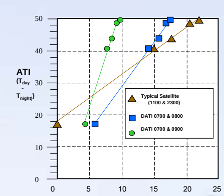

Figure 10: ATI vs 3 different DATI for surfaces with different P. Note the linear relationship between ATI and DATI.

- The next step in this study is to convert this rate into predicted day/night apparent thermal inertia and then to estimate thermal inertia.

References

Gillespie, A.R., and Kahle, A., 1977. The construction and interpretation of a digital thermal inertia image. *Photogrammetric Engineering and Remote Sensing* 43(8), 983-1000.

Kahle, A., 1977. A simple thermal model of the Earth's surface for geologic mapping by remote sensing. *Journal of Geophysical Research* 82, 1673-1680.

Kahle, A., 1980. Surface Thermal Properties. *In* Remote Sensing in Geology, Siegal, B.S., and Gillespie, A.R. *eds*., John Wiley & Sons, N.Y., N.Y., pp. 227-273.

Price, J.C., 1977, Thernal inertia mapping: A new view of the earth. *J. Geophys. Res.*, 82, 2582-2590.

Van Dam, R., Borchers, B., and Hendricks, J., 2005, Strength of landmine signatures under different soil conditions: implications for sensor fusion. *International Journal of Systems Science, Special Issue on Robots and Sensors for Landmine Detection*, 36(9), 573-588.

Acknowledgments

This study is sponsored by the Department of the Army, Army Research Office (ARO contract number DAAD19-03-1-0159); the content of the information does not necessarily reflect the position or the policy of the federal government.